Science of the Total Environment 906 (2024) 167643

Contents lists available at ScienceDirect

Science of the Total Environment

journal homepage: www.elsevier.com/locate/scitotenv

Seasonal riverine inputs may affect diet and mercury bioaccumulation in Arctic coastal zooplankton

Nathalie Carrasco [a,b,c,*], Maeve McGovern [c], Anita Evenset [d], Janne E. Søreide [e], Michael T. Arts [f], Sofi Jonsson [g], Amanda E. Poste [a,c,h,**]

[a] Department of Arctic Marine Biology, UiT, The Arctic University of Norway, 9019 Tromsø, Norway
[b] Oceanographic Institute - Prince Albert I Foundation, 98000, Monaco
[c] Norwegian Institute for Water Research, 9007 Tromsø, Norway
[d] Akvaplan-niva, Fram Centre, 9007 Tromsø, Norway
[e] University Centre in Svalbard, 9170 Longyearbyen, Norway
[f] Toronto Metropolitan University, Toronto M5B 2K3, Canada
[g] Department of Environmental Science, Stockholm University, SE-106 91 Stockholm, Sweden
[h] Norwegian Institute for Nature Research, 9296 Tromsø, Norway

HIGHLIGHTS

- River inputs over the season affected surface water physicochemistry in an Arctic coastal estuary.
- Zooplankton $\delta^{13}C$ values reflected terrestrial carbon utilization during the main river discharge period.
- [Hg] in zooplankton increased following higher river discharge and shifts in diet and community structure.

GRAPHICAL ABSTRACT

Conceptual figure summarizing Hg concentrations in zooplankton from April to August 2018 alongside changes in river discharge and tOM contribution to zooplankton diet.

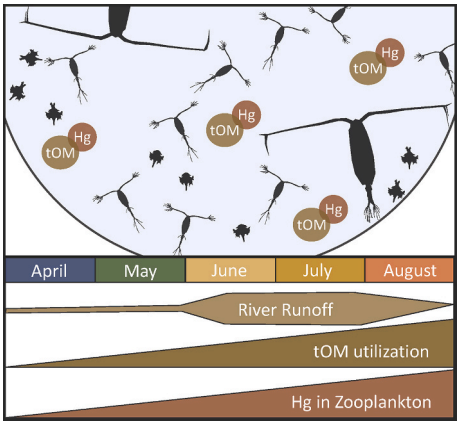

ARTICLE INFO

Editor: Daniel Wunderlin

Keywords:
Arctic estuaries
Climate change

ABSTRACT

Climate change driven increases in permafrost thaw and terrestrial runoff are expected to facilitate the mobilization and transport of mercury (Hg) from catchment soils to coastal areas in the Arctic, potentially increasing Hg exposure of marine food webs. The main aim of this study was to determine the impacts of seasonal riverine inputs on land-ocean Hg transport, zooplankton diet and Hg bioaccumulation in an Arctic estuary (Adventfjorden, Svalbard). The Adventelva River was a source of dissolved and particulate Hg to Adventfjorden,

* Correspondence to: N. Carrasco, Oceanographic Institute - Prince Albert I Foundation, 98000, Monaco.
** Correspondence to: A.E. Poste, Norwegian Institute for Nature Research, 9296 Tromsø, Norway.
E-mail addresses: n.carrasco@oceano.org (N. Carrasco), amanda.poste@nina.no (A.E. Poste).

https://doi.org/10.1016/j.scitotenv.2023.167643
Received 26 July 2023; Received in revised form 17 September 2023; Accepted 5 October 2023
Available online 6 October 2023

Fatty acids
Mercury
River inputs
Stable isotopes
Terrestrial organic matter
Zooplankton diet

especially in June and July during the river's main discharge period. Stable isotope and fatty acid analyses suggest that zooplankton diet varied seasonally with diatoms dominating during the spring phytoplankton bloom in May and with increasing contributions of dinoflagellates in the summer months. In addition, there was evidence of increased terrestrial carbon utilization by zooplankton in June and July, when terrestrial particles contributed substantially to the particulate organic matter pool. Total (TotHg) and methyl Hg (MeHg) concentrations in zooplankton increased from April to August related to increased exposure to riverine inputs, and to shifts in zooplankton diet and community structure. Longer and warmer summer seasons will probably increase riverine runoff and thus Hg exposure to Arctic zooplankton.

1. Introduction

Most anthropogenic mercury (Hg) in the Arctic originates from long-range transport (i.e. comes from the atmosphere and/or the ocean) rather than from point-source emissions (AMAP, 2021). Current estimates suggest that permafrost soils in the Northern Hemisphere contain 67 Gg Hg (i.e. 67,000 t) (Lim et al., 2020), which makes them a globally significant pool (Ariya et al., 2004; Macdonald and Loseto, 2010; Olson et al., 2018; Schuster et al., 2018). Climate change is leading to increased mobilization and transport of Hg from permafrost catchments to coastal waters (Dommergue et al., 2003; Emmerton et al., 2013; Olson et al., 2018; Schuster et al., 2018), with elevated Hg concentrations reported for water, sediment, soil and biota from different Arctic regions, including Svalbard (Lehnherr, 2014; Halbach et al., 2017). However, the fate of terrestrially-derived Hg in the coastal environment, and the potential for increased accumulation of Hg in coastal biota remains poorly documented.

Contaminant uptake in the food web depends on the biomass at its base at the time of peak inputs, and also on contaminant bioavailability. Methyl mercury (MeHg), the most toxic form of Hg, has a greater potential for bioaccumulation and biomagnification than inorganic Hg (Morel et al., 1998; Kuhnlein and Chan, 2000; Clarkson et al., 2003). In aquatic systems, availability of organic matter substrate and anoxic conditions in the water column and sediments are known to promote the transformation of inorganic Hg into MeHg, by a broad range of microorganisms (Gilmour et al., 2013; Gagnon et al., 1996; Morel et al., 1998). However, recent evidence also points to the potential for methylation under oxic conditions in Arctic marine waters, including in stratified river-influenced surface waters (Schartup et al., 2015b). Furthermore, climate change-mediated increases in the transport of terrestrially-derived organic material and sediments from catchments to coastal surface waters have the potential to alter physico-chemical conditions (McGovern et al., 2020a), with implications for contaminant uptake and bioaccumulation (McGovern et al., 2019).

Sediment and organic matter-rich freshwater inputs, which drive the rapid attenuation of light needed for photosynthesis (McGovern et al., 2020a), have the potential to increase the importance of heterotrophic and terrestrial food sources to higher-trophic level organisms (Andersson et al., 2018, McGovern et al., 2023 in prep). However, bacterial and terrestrially-derived organic matter are lower in nutritional quality than phytoplankton (Hiltunen et al., 2019). Because aquatic food webs with a strong microbial loop component (and hence an increased reliance of zooplankton on heterotrophic food sources) have additional trophic transfers compared to phytoplankton-based food webs, such conditions may increase concentrations of biomagnifying contaminants such as MeHg in consumer organisms (Jonsson et al., 2017). In addition, the lower dietary quality to zooplankton of terrestrial organic matter sources, e.g. with higher C:N ratios and lower levels of polyunsaturated (PUFA) and essential fatty acids (EFA) required for optimal growth and development, can lead to decreased trophic efficiency through marine food webs (Arts et al., 2009), which can in turn lead to less growth dilution of MeHg. Furthermore, dietary exposure is the main pathway through which higher trophic level species are exposed to MeHg (Hall et al., 1997). Thus, seasonal variability in zooplankton diet may have an impact on the uptake of Hg at the base of the marine food web. Despite this, no studies (to our knowledge) have focused on seasonal diet variability and Hg bioaccumulation in zooplankton in river-influenced Arctic coastal waters.

The overarching aim of this study was thus to understand how seasonal river inputs affect diet and mercury bioaccumulation in coastal zooplankton. We hypothesized that river inputs would be a significant source of terrestrial carbon and Hg to the fjord system, and that increased Hg exposure at the base of the food web and utilization of terrestrial and heterotrophic food sources by fjord zooplankton, would be associated with significantly increased concentrations of total Hg (TotHg) and MeHg in lower trophic levels during the summer riverine runoff period.

2. Materials and methods

2.1. Field sampling

The current study was carried out in Adventfjorden, a small fjord arm (max. Depth = 90 m) of Isfjorden located in West Spitsbergen, Svalbard (Fig. 1). Isfjorden is an open fjord which is influenced by the relatively warm and saline West Spitsbergen Current (WSC) a continuation of the North Atlantic Current, and the colder and less saline East Spitsbergen Current (Arctic Ocean water) originating from East Svalbard, which both flow northwards along West Spitsbergen (Nilsen et al., 2008; Skogseth et al., 2020). The inner part of Adventfjorden is a shallow estuary which receives significant freshwater input from the Adventelva River, which transports meltwater from upstream glaciers (Zajączkowski and Włodarska-Kowalczuk, 2007; Zajaczkowski, 2008; Zajaczkowski et al., 2010), and runoff from precipitation and snowmelt. Few quantitative data are available on riverine inputs to Adventfjorden, but during summer 2001, the discharge in the Adventelva River was estimated to reach a maximum of 3.6 $m^3 s^{-1}$ (Zajaczkowski, 2008). Zooplankton and seawater samples were collected monthly from April to August 2018 at 3 stations along a gradient from inner to outer Adventfjorden (AF1, AF2 and IsA; Fig. 1). In addition, surface water was collected from the Adventelva River monthly between May and August (Fig. 1). At each fjord station, a CTD profiler (SD204, SAIV A/S) was used to collect vertical profiles of salinity and temperature. Furthermore, seawater was collected from a Niskin bottle at 2 depths: just below surface and at 15 m. Turbidity was measured from each water sample in the field using a Thermo Eutech TN-100 turbidity meter. Water for filtration was stored in high-density polyethylene (HDPE) containers under dark and cold conditions until processing at the University Centre in Svalbard as soon as possible after collection (within 4 h). Zooplankton were sampled with integrated vertical hauls from 2 m above the bottom to the surface. In order to collect zooplankton from different size classes, 60 and 200 μm WP2 nets (both with a diameter of 0.25 m^2) and a larger and coarser 1000 μm WP3 net (with a diameter of 1 m^2) were used. All net haul material was pooled and macrozooplankton (e.g. euphausiids, *Themisto* spp., jellyfish) were removed before the remaining mesozooplankton were size-fractionated using sequential Nitex mesh screens with mesh sizes of 1000, 500, 200, and 50 μm. Because macrozooplankton taxa (> 1000 μm) differed substantially among stations and dates, we chose to focus on size fractionated mesozooplankton (between 50 and 1000 μm) in this study. From each of the size-fractionated samples, subsamples

were taken for species identification (fixed with 4 % formalin-seawater solution buffered with Borax®), stable isotope and Hg analysis (frozen at −20°C), and fatty acid analysis (frozen at −80°C).

2.2. Water chemistry

For determination of suspended particulate matter (SPM) concentrations, water samples (seawater $n = 28$; rivers $n = 4$; Table S1 in the Supplementary material) were filtered onto pre-weighed (oven-dried at 60°C for 1 h) 47 mm Whatman QMA quartz fibre filters (for determination of particulate Hg concentrations on a mass basis) and were stored at −20°C. SPM concentrations (mg/L) were determined gravimetrically at the University Centre in Svalbard.

For Chlorophyll-*a* (Chl-*a*) analysis, water samples from the fjord were filtered onto 25 mm GF/F filters that were wrapped in aluminium foil and stored at −80°C until analysis. Chl-*a* was analyzed at the University Centre in Svalbard (n = 28). Chl-*a* was extracted from filters with 10 mL of 100 % methanol in the dark at 4°C for 20–24 h (Holm-Hansen and Riemann, 1978), and fluorescence was determined using a 10-AU-005-CE Fluorometer (Turner, USA). After measuring total Chl-*a*, the fraction of phaeopigments was determined by the addition of 5 % HCl, followed by an additional fluorescence measurement (Parsons, 2013).

2.3. Zooplankton identification

The relative contribution of different zooplankton taxa to the total biomass of size-fractionated samples was estimated by pairing sample identification through microscopy with previously reported taxon-specific estimates of dry weights for individuals of Arctic zooplankton (Blachowiak-Samolyk et al., 2008 and references therein). Individuals were identified, measured and counted. In size fractions containing few organisms (i.e. <200), all individuals were identified. In size fractions with high zooplankton abundance, the sample was diluted in 100 mL of seawater and 2 mL sub-samples were analyzed, until 200 individuals had been counted. The relative abundance and biomass of zooplankton taxa were then calculated within each size fraction.

2.4. Dietary markers

For stable isotope analysis (SIA) of particulate organic matter (POM), river and fjord water were filtered onto pre-combusted 25 mm Whatman GF/F filters, which were then wrapped in aluminium foil and frozen at −20°C until analysis. Analysis of stable isotopes of carbon ($\delta^{13}C$) and nitrogen ($\delta^{15}N$) and determination of carbon and nitrogen content, was carried out for POM and zooplankton at the University of California, Davis (UC Davis Stable Isotope Facility, USA). Prior to analysis, both POM filters ($n = 28$; Table S1 in the Supplementary material) and zooplankton samples ($n = 34$; Table S1 in the Supplementary material) were freeze-dried for 24–48 h. POM filters were then packed in tin capsules. Zooplankton samples were homogenized using an agate mortar and pestle. A sub-sample was then weighed to the nearest 1 μg using a Mettler Toledo balance and packed in tin capsules. Because $\delta^{13}C$ measurements can be influenced by carbonate content (Bodin et al., 2007), two parallel filters for POM were analyzed, one unacidified and one acidified (for carbonate removal). A subset of acidified zooplankton samples ($n = 16$) were also analyzed in parallel to test for effects of acidification on zooplankton $\delta^{13}C$. Although there was a significant difference between acidified and unacidified POM samples (Paired *t*-

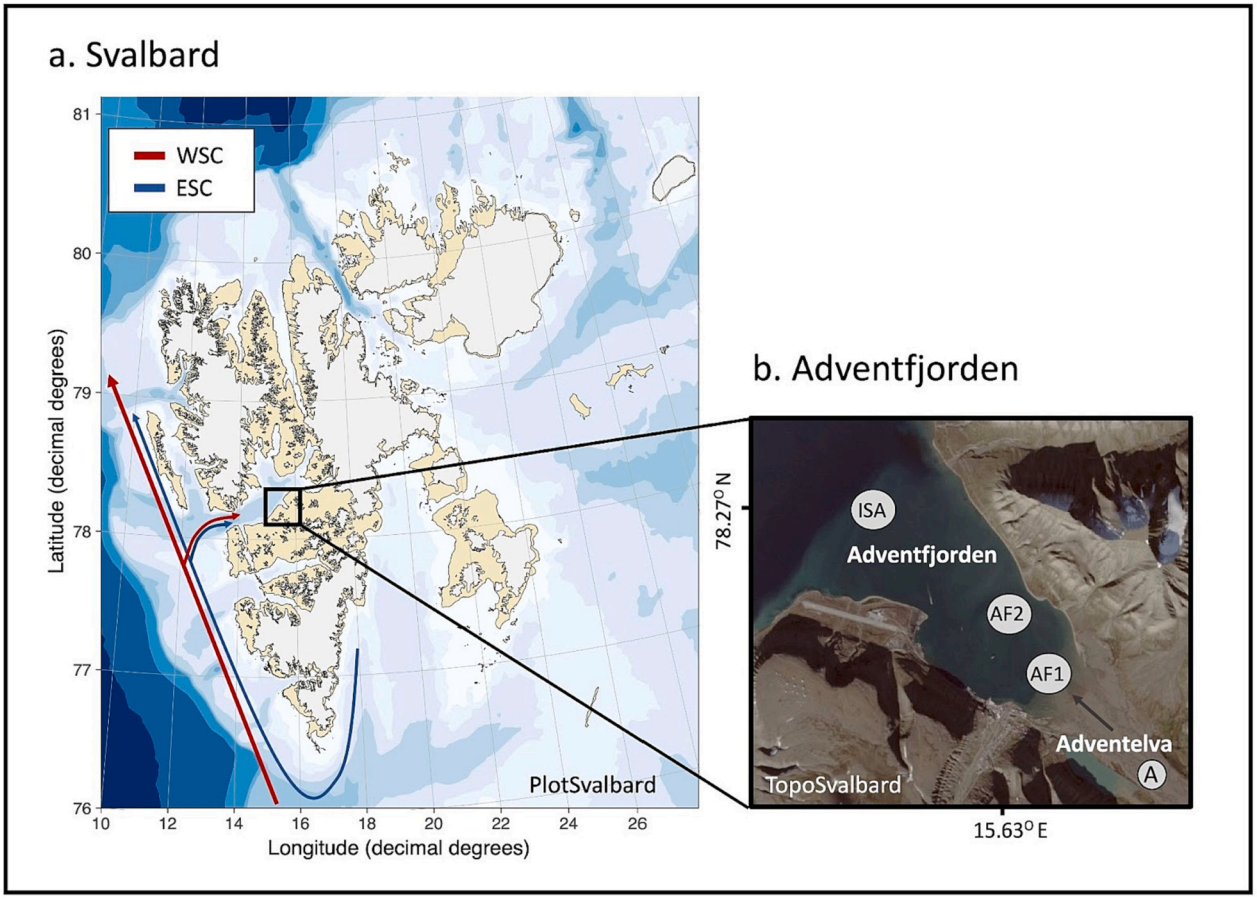

Fig. 1. (a) Map of Svalbard with the West Spitsbergen Current (WSC) and East Spitsbergen Current (ESC). (b) Adventfjorden with sampling locations shown with circles: river station Adventelva (A) and the fjord stations (AF1, AF2, IsA).

test, $p < 0.001$), this was not the case between acidified and unacidified zooplankton samples. Hence, acidified POM samples provided $\delta^{13}C$ values and particulate organic carbon (POC) content and unacidified ones provided $\delta^{15}N$ values, and particulate nitrogen (PartN) and carbon (PartC) content. Data from unacidified zooplankton samples were used for further data analysis. $\delta^{13}C$, $\delta^{15}N$, and C and N content were analyzed using an Elementar Vario EL Cube or Micro Cube elemental analyser (Elementar analysensysteme GmbH, Hanau, Germany) interfaced to an PDZ Europa ANCA-GSL elemental analyser interfaced to a PDZ Europa 20–20 continuous flow isotope ratio mass spectrometer (IRMS), (Sercon Ltd., Cheshire, UK) for POM samples; while zooplankton samples were analyzed using an PDZ Europa ANCA-GSL elemental analyser interfaced to a PDZ Europa 20–20 continuous flow isotope ratio mass spectrometer (IRMS), (Sercon Ltd., Cheshire, UK). Standard deviation for reference materials ranged from ±0.01 to ±0.08 ‰ for $\delta^{13}C$, and ± 0.01to ± 0.03 ‰ for $\delta^{15}N$ for sample runs that included acidified samples; and from ±0.03 to ±0.13 ‰ for $\delta^{13}C$, and ± 0.03 to ±0.04 ‰ for $\delta^{15}N$ for sample runs that included unacidified samples.

$\delta^{13}C$ and $\delta^{15}N$ values are expressed in delta notation:

$$\delta X = [Rsample/Rstandard) - 1] \times 1000 \quad (1)$$

expressed in units of per thousand (‰) and where X is C or N, and R is $^{13}C/^{12}C$ or $^{15}N/^{14}N$ of the sample or the standard (Pee Dee Belemnite limestone for C and atmospheric N_2 for N).

Fatty acid (FA) analysis was carried out for a subset of zooplankton size-fractionated samples ($n = 24$; Table S1 in the Supplementary material) at Toronto Metropolitan University (formerly Ryerson University, Toronto, Canada) broadly following methods outlined in Folch et al. (1957). Total lipids were extracted with 4 mL of 2:1 chloroform:methanol. 18 μg of Tricosanoic acid (23:0) was added to each tube as an internal standard for estimating recovery and methylation efficiency (mean ~ 80 %). The extracts were then dried with non-reactive, extra-dry, nitrogen gas. For the methylation of FA, 2 mL of hexanes was added to each of the tubes after which two 100 μL aliquots of the lipid solution was removed from each tube and placed in cast tin cups. After evaporation of the solvent, the tubes were placed on a heating block for 90 min at 90°C. A Shimadzu GC-2010 plus, with an AOC-20i/s auto-sampler and twin auto-injectors, with Shimadzu LabSolutions software, was used to quantify FA. Column temperature was set to: hold at 140°C for 5 min, ramp up to 240°C at 2°C/min for 50 min, and then hold at 240°C for the final 10 min. FA in each samples were identified and quantified by referencing them to the retention times of FA and using a series of calibration standards (GLC 463, GLC 68E, and 23:0, NuChek Prep., Waterville, MN, USA). In total, 42 fatty acids were analyzed and 4 fatty acid trophic markers (FATM) were included for further statistical analysis (Table S2 in the Supplementary material).

2.5. Hg analysis

Dissolved TotHg (DTotHg) samples were collected from 0.2 μm filtrate (polycarbonate Millipore filters) and then frozen at −20°C until analysis. Analysis of DTotHg was carried out at the Norwegian Institute for Water Research (NIVA). TotHg was determined through oxidation, purge and trap and cold vapor atomic fluorescence spectrometry (CVAFS) based on USEPA method 1631 (US EPA, 1999). For analysis of particulate TotHg (PartTotHg), river and fjord water were filtered onto pre-combusted (trace metal clean) 25 mm Whatman QMA quartz fibre filters, and stored in aluminium foil at −20°C until analysis. TotHg analysis for PartTotHg (River $n = 4$; Fjord $n = 28$; Table S1 in the Supplementary material) and TotHg in zooplankton (n = 28 homogenized samples where mass was sufficient for analysis; ~10 mg; Table S1 in the Supplementary material) was carried out using a Direct Mercury Analyser (DMA-80) at Akvaplan-niva in Tromsø, Norway (U.S.E.P.A). Quality assurance measures included 3 blanks (1st run: 0.03 ± 0.01 ng, 2nd run: 0.03 ± 0.02 ng for POM samples, and 1st run: 0.05 ± 0.02 ng, 2nd run: 0.04 ± 0.02 ng for zooplankton samples), 3 blank analytical boats (1st run: 0.02 ± 0 ng, 2nd run: 0.02 ± 0 ng for POM samples and 1st run: 0.02 ± 0.01 ng, 2nd run: 0.01 ± 0 ng for zooplankton samples) and 3 blank filters for POM (1st run: 0.01 ± 0 ng, 2nd run: 0.01 ± 0 ng), and analysis of reference materials (CRM-DORM-4, fish protein, National Research Council Canada) (n = 2 for each run) to assess precision. CRMs were always within the certified concentration range (416 ± 28 ng/g).

MeHg analysis in zooplankton was carried out at Stockholm University (SU), Sweden for samples which had sufficient mass for analysis (0.05–0.1 g; $n = 33$; Table S1 in the Supplementary material). The procedure for preparation and analysis of MeHg was based on the method described by Hintelmann and Nguyen (2005) and Braaten et al. (2014) with minor adjustments. Briefly, freeze-dried and homogenized samples (same as those used for stable isotope analysis) were weighed out into Falcon tubes and digested using trace-metal grade nitric acid (30 % *v*/v) (Fisher Scientific) in a 60°C bath for 16–17 h. After acid digestion, the samples were analyzed using a 2700 Methyl Mercury Auto-Analysis System (Tekran, Canada). Quality assurance measures included method blanks (0.01 ± 0.002 ng/L), analysis of certified reference materials (CRM-DORM-4, $n = 6$; National Research Council Canada and TORT-2, n = 3; National Research Council Canada), matrix spikes (n = 6; recoveries ranged from 85 to 100 %) and sample replicates (n = 6; relative % difference ranged from 1.5 to 35 %). CRMs were always within the certified concentration range.

2.6. Data treatment and statistical analysis

Lipid correction of $\delta^{13}C$ values in zooplankton is often necessary to account for seasonality and interspecific differences in lipid concentration, since lipids have very low $\delta^{13}C$ values (Hobson and Clark, 1992). $\delta^{13}C$ values in zooplankton were lipid-corrected using C:N ratio according to the model in Pomerleau et al. (2014).

$$\delta^{13}CLEA = \delta^{13}Cbulk + \Delta^{13}C \quad (2)$$

where $\delta^{13}CLEA$ is $\delta^{13}C$ lipid-extracted and acidified; $\delta^{13}C$ bulk refers to raw $\delta^{13}C$ values for zooplankton and $\Delta\ ^{13}C$ calculated as:

$$\Delta^{13}C = (0.206^{*}C : N) + 2.02 \quad (3)$$

All statistical analyses were carried out in R (version 4.3.1; R Core Team, 2023) using RStudio. Given the small dataset with many covariate variables, and the strong seasonality of the data, we chose to focus on univariate analysis and Principal Component Analysis (PCA), rather than General Linear Model, constrained ordination or mixing model analysis. Since data for most zooplankton and water chemistry parameters were non-normally distributed (confirmed by Shapiro-Wilk tests), the non-parametric Kruskal-Wallis test and pairwise comparisons using Wilcoxon rank sum were used to test differences in water chemistry, Hg loading, dietary markers and contamination of zooplankton among months, stations and size-fractions. Furthermore, PCA was used to explore correlations, similarities and differences between physicochemical data, dietary markers ($\delta^{13}C$, FA), and TotHg and MeHg concentrations as well as MeHg:TotHg ratio (%MeHg) in zooplankton. In addition, Spearman's rank correlations were used to examine correlations between physicochemical parameters, diet, community, and TotHg and MeHg concentrations in zooplankton.

3. Results

3.1. Physicochemical conditions in the Adventelva River and Adventfjorden

The Adventelva River started flowing in May, with the highest water level observed in late June to early August (A. Poste unpublished data). SPM concentrations in the Adventelva River ranged from 137 to 204

mg/L over the season with highest values in August. DTotHg concentrations in the Adventelva River were highest in May (0.6 ng/L), with concentrations of 0.2 and 0.1 ng/L observed in June and August, respectively. PartTotHg concentrations increased through the melt season, with the highest concentrations measured in August (13 ng/L). In general, TotHg in river water samples was highly particle associated, with 94, 97 and 99 % of TotHg in the particulate fraction in May, June and August respectively. While SPM in the Adventelva River increased with discharge, TotHg concentrations showed a seasonal increase from April to August even when normalized for SPM (SPM-normalized TotHg ranged from 50 to 63 ng/g SPM) (Fig. 2).

Freshwater inputs to Adventfjorden resulted in strong gradients in physicochemical conditions in surface waters. The inner part of Adventfjorden (AF1) was characterized by a fresh, turbid surface layer in June and July, with salinities as low as 7.26 PSU at 50 cm depth in June. The outermost station (IsA) was also freshwater influenced during the summer period, especially in July and August with mean salinities of 31.6 and 32.7 PSU, respectively, in the surface 3 m (Fig. S1 in the Supplementary material). Freshwater influenced stations were also characterized by relatively high SPM concentrations (22–156 ng/L) and molar C:N ratios (9–41), especially in June and July, as well as increased concentrations of PartTotHg and DTotHg (Fig. S2 in the Supplementary material). DTotHg concentrations exceeded 0.1 ng/L in the surface waters of the inner fjord in May, for surface and deep waters from the inner (AF1) and mid-fjord (AF2) stations in June, and for a single surface water sample from AF2 in August. All other samples had concentrations ranging from 0.03 to 0.09 ng/L. Over the study period, PartTotHg concentrations in Adventfjorden ranged from 0.06 to 8.1 ng/L with the highest values in the inner fjord in June and July. The proportion of TotHg present in the particulate phase ranged from 30 to 93 % over the season, with the lowest value observed in May at the outermost station (IsA) and the highest value observed in July in the inner part of Adventfjorden (AF1). Meanwhile, when normalized for SPM, TotHg concentrations in surface waters ranged from 1.97 to 85.69 ng/g with the highest values recorded in June and July at the innermost station (Fig. 2).

3.2. Zooplankton community

Calanus spp. dominated the biomass in the largest size fractions (500–1000 μm) during the entire study period, except in May when the zooplankton size-fractionated samples were dominated by meroplankton (Decapod zoea and Cirripedia nauplii) (Fig. S3 in the Supplementary material.). In the smallest size fractions, *Oithona similis* dominated the biomass in April and August. In August, the "Other" category was dominated by copepod nauplii, but also included many bivalve and echinoderm larvae, as well as *Microcalanus* spp., *Oithona atlantica*, *Oikopleura*, and *Pseudocalanus* spp..

3.3. Stable isotopes

For POM from the Adventelva River, $\delta^{13}C$ values ranged from −25.4 to −26.8 ‰ and $\delta^{15}N$ values ranged from 1.5 to 3.3 ‰ over the study period (Fig. 3 A&C). In nearby Adventfjorden surface waters, $\delta^{13}C$-POM values ranged from −33.5 to −22.8 ‰, with values more enriched in ^{13}C in May (Kruskal-Wallis $p < 0.01$; Pairwise Wilcoxon $p = 0.02$) and more depleted in ^{13}C in the outer fjord in April (Fig. 3A). The $\delta^{15}N$ values ranged from 2.9 to 6.8 ‰ and decreased throughout the study period (Kruskall-Wallis; p = 0.02; Fig. 3C). There were no significant differences between stations sampled the same day, except for $\delta^{13}C$ values in April, which were lower in outer fjord (Kruskal-Wallis; $p < 0.05$).

In addition, there were no significant differences between stations or between size-fractions in zooplankton $\delta^{13}C$ and $\delta^{15}N$ values (Kruskal-Wallis, $p > 0.1$; $p > 0.03$) for samples collected on the same date. $\delta^{13}C$ values ranged from −24.9 to −17.8 ‰ with values significantly more enriched in ^{13}C in May than in April, June, July and August (Kruskal-

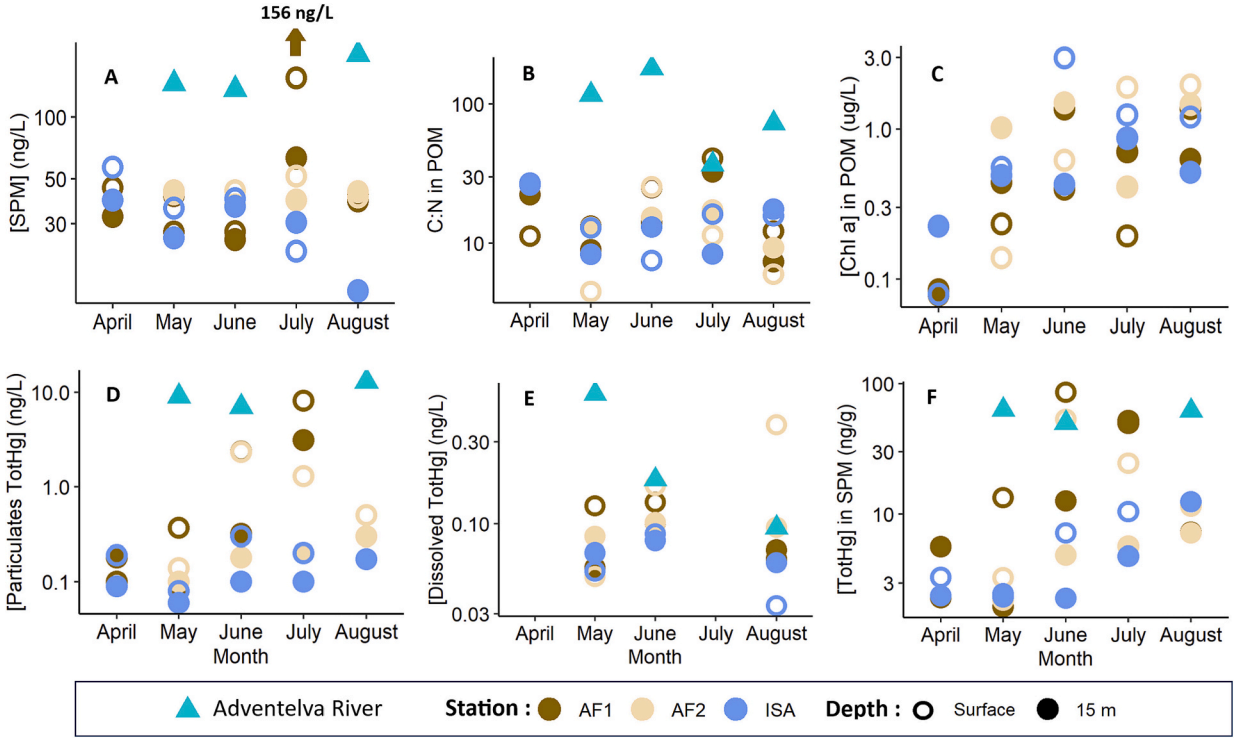

Fig. 2. Scatter plots for selected water chemistry parameters for the Adventelva River ($n = 4$) and the 3 stations in Adventfjorden (AF1, AF2, and IsA; $n = 28$ in total). River samples were collected from May to August, while seawater samples were collected from April to August. Data shown include: (A) SPM, (B) Molar C:N ratio, (C) Chl-*a* concentration, (D) PartTotHg concentration, (E) DTotHg concentration and (F) TotHg concentration per gram SPM. Data are shown on a log axis. The highest SPM concentration observed in July is highlighted with an up arrow and its value.

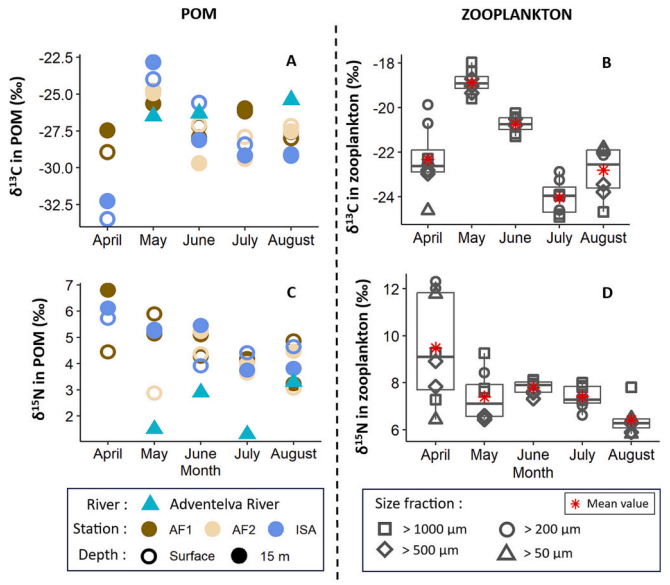

Fig. 3. Stable isotope ($\delta^{13}C$ and $\delta^{15}N$) values for POM (A&C, Fjord $n = 28$; River $n = 4$) and size fractionated bulk zooplankton samples (B&D, $n = 34$; zooplankton size fractions are represented by symbols) collected in the Adventelva River and at the 3 stations in Adventfjorden from April to August 2018.

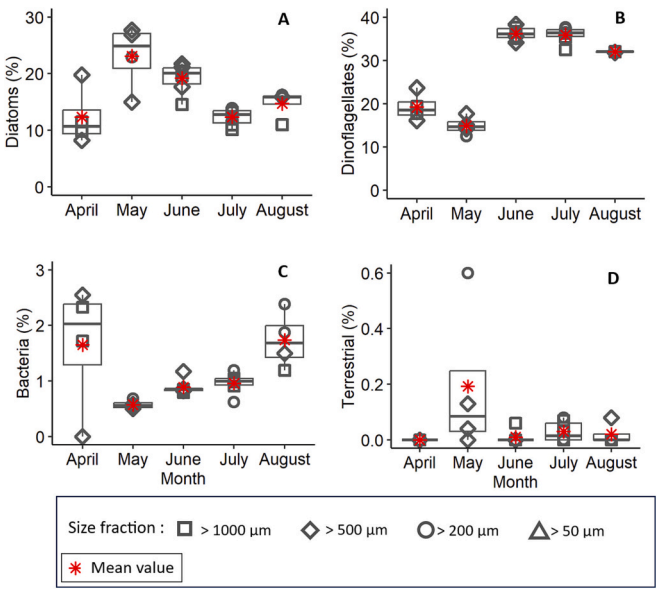

Fig. 4. Boxplots for FATM, including (A) Diatom (16:1n-7 + 20:5n-3), (B) Dinoflagellates (∑C18PUFA + 22:6n-3), (C) Bacteria (∑Odd-chain) and (D) Terrestrial material (22:0 + 24:0) in size-fractionated zooplankton samples ($n = 24$; zooplankton size fractions are represented by symbols) collected at the 3 stations in Adventfjorden from April to August 2018.

Wallis $p < 0.01$; Pairwise Wilcoxon $p < 0.01$) (Fig. 3B). $\delta^{15}N$ values ranged from 5.8 to 12.3 ‰, and while there were no significant differences between sampling dates, there was a clear seasonal trend with gradually lower $\delta^{15}N$ from April to August (Fig. 3D).

Overall, zooplankton from all stations were enriched in ^{13}C and ^{15}N relative to POM for all months. $\delta^{13}C$ values in zooplankton samples followed the same seasonal trajectory as $\delta^{13}C$ of POM with the highest values in May and the lowest values in April, July and August (Fig. 3B&D; Fig. S4 in the Supplementary material). However, the magnitude of the change in stable isotope values for POM was larger than the seasonal changes observed for zooplankton.

3.4. Fatty acid composition of zooplankton

No significant differences in FA trophic markers were found between stations or zooplankton size fractions within the same month of sampling (Kruskal-Wallis, $p > 0.05$). Across months, however, relatively large differences in zooplankton FATM were found (Fig. 4). The contribution of the diatom FATM to total lipids in zooplankton peaked in May (23 ± 5 %) and then decreased during the following months (Fig. 4A). This decrease in diatom FATM was accompanied by an increase in the contribution of dinoflagellate markers in June (36 ± 1 %), July (36 ± 2 %) and August (32 ± 1 %) (Kruskal-Wallis, $p < 0.01$) (Fig. 4B). Meanwhile, bacterial FATM, which were high in April (1.6 ± 1 %), showed consistent increases through the melt season from May to August (Kruskal-Wallis, $p = 0.01$), with the highest proportions during the run-off season in August (1.7 ± 0.4 %) across all size fractions and stations in Adventfjorden (Fig. 4C). Terrestrial FATM proportions remained very low and constant during the entire study period ranging from 0.03 to 0.6 % (Fig. 4D). The proportion of SFA and MUFA decreased significantly (Kruskal-Wallis, $p < 0.01$) through the summer months from 34 % in April to 24 % in August while the proportion of PUFA increased and was highest (up to 62 % of total lipids) in June, July and August (Kruskal-Wallis, $p < 0.01$).

3.5. TotHg and MeHg in zooplankton

TotHg and MeHg concentrations in zooplankton were not significantly different between stations (Kruskal Wallis $p > 0.05$), or between zooplankton size fractions sampled on the same date (Kruskal Wallis $p > 0.05$). TotHg concentration in zooplankton samples ranged from 1.3 to 15.1 ng/g, with the lowest values in April (Kruskal-Wallis $p < 0.01$; Pairwise Wilcoxon $p < 0.01$) (Fig. 5A). MeHg concentration in zooplankton samples ranged from 0.02 to 3.9 ng/g, with the lowest values in April and May, and the highest values in July and August (Kruskal-Wallis $p < 0.01$; Pairwise Wilcoxon $p < 0.01$) (Fig. 5B). %MeHg ranged from 0.5 to 24 % with highest values in July and August (Fig. 5C).

Hg concentrations in zooplankton were related to water chemistry, dietary markers and community composition. TotHg concentrations in zooplankton were positively correlated with PartTotHg and DTotHg concentrations in surface water, turbidity, as well as dinoflagellate FATM and were negatively correlated with salinity. MeHg concentrations and %MeHg in zooplankton were positively correlated with the dinoflagellate and bacteria FATM and negatively correlated with the diatom marker and $\delta^{13}C$ in zooplankton samples. In addition, %MeHg was negatively correlated with %meroplankton in each size fraction sample (Fig. S5 in the Supplementary material). The PCA further illustrated the relationships between TotHg and MeHg concentrations in zooplankton and changes in water chemistry and dietary markers. PC1 explained 47 % of the variability in the dataset and was driven by changes in river run-off, with April and May (before run-off) to the left, and June, July and August (the melt season) to the right. Concentrations of PartTotHg and DTotHg in the water column were strongly correlated with PC1, demonstrating the importance of river inputs for delivering Hg to Adventfjorden's surface waters. Furthermore, zooplankton samples collected in July and August were characterized by relatively high MeHg and TotHg concentrations, alongside the observed increases in the dinoflagellate dietary marker. PC2 explained 25 % of the variability of the dataset and was driven by differences within these two main periods of the field season (i.e. before and after the start of river runoff). The bacterial FATM was strongly related to the second axis, indicating that bacteria are an important food source both during pre-spring bloom and late-summer conditions (Fig. 6).

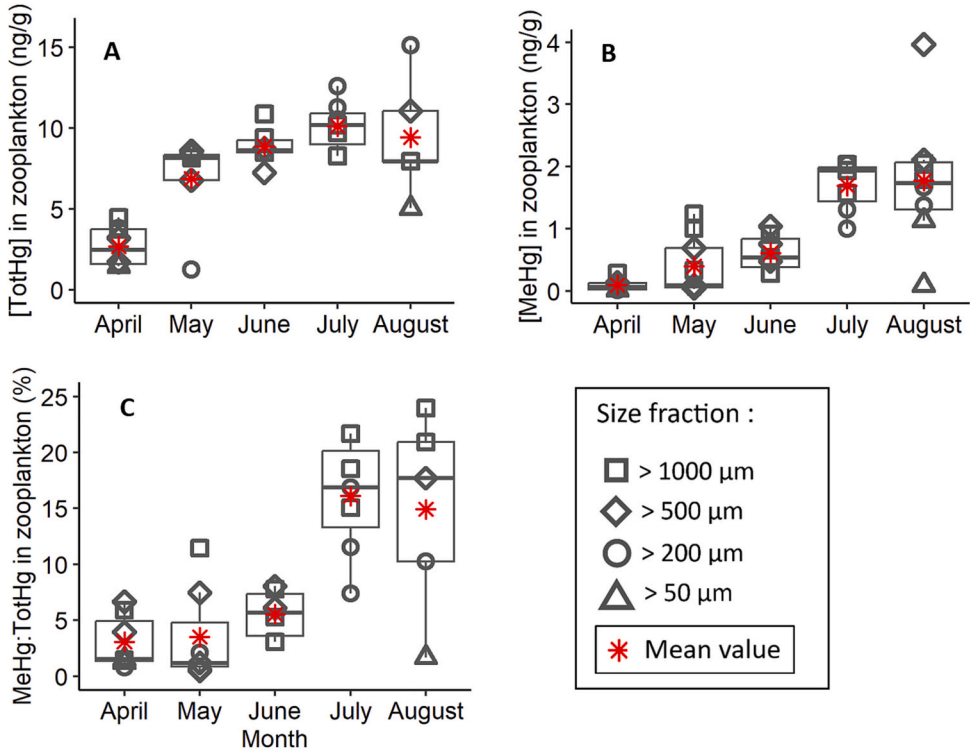

Fig. 5. Boxplots of Hg concentrations for zooplankton samples (TotHg $n = 28$; MeHg $n = 33$; zooplankton size fractions are represented by symbols) collected at the 3 stations in Adventfjorden from April to August 2018. Data shown include (A) TotHg, (B) MeHg and (C) %MeHg in zooplankton samples.

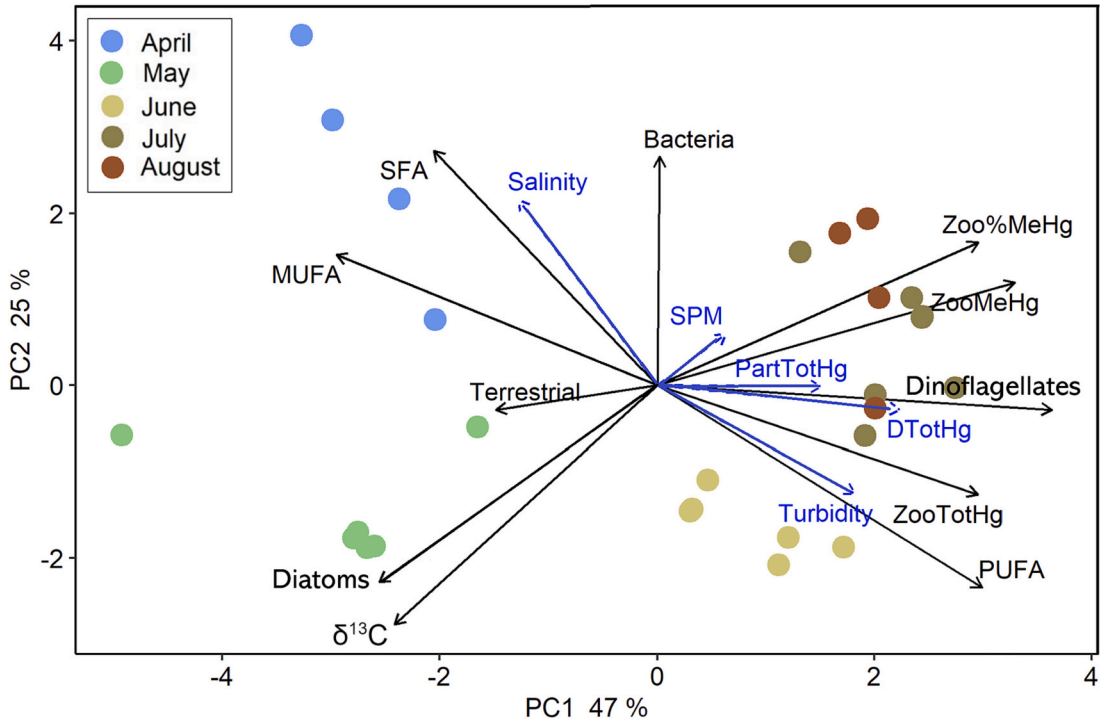

Fig. 6. Principal component analysis (PCA) based on TotHg, MeHg and %MeHg in zooplankton as well as $\delta^{13}C$, SFA, MUFA, FATM (for bacteria, dinoflagellates, diatoms and terrestrial material) in zooplankton ($n = 25$). Salinity, turbidity, SPM, as well as DTotHg and PartTotH in water samples, are included as passive vectors (in blue). The two first components explained 72 % of the total variance. Dots represent the average score of zooplankton samples, whereas arrows represent the direction of importance for the measured parameter in separating the samples.

4. Discussion

4.1. Freshwater influence in Adventfjorden

Freshwater inputs from the Adventelva River had a strong impact on physicochemical conditions in fjord surface waters during the summer months. The freshwater footprint in Adventfjorden was characterized by low salinity and high turbidity as well as high concentrations of SPM. This fresh, turbid surface layer was extensive in June, July and August, and was detectable even at the outermost sampling station IsA (~ 7 km from the river mouth). The high suspended sediment loads associated with river run-off rapidly attenuate light needed for photosynthesis (Retamal et al., 2008; Hessen et al., 2010; McGovern et al., 2020a), and thus can negatively impact marine phytoplankton production (Retamal et al., 2008; Hessen et al., 2010). In addition, these freshwater inputs can also transport terrestrially-derived organic carbon and Hg from catchment soils to coastal surface waters (Schuster et al., 2011; Zolkos et al., 2020). The distinctly terrestrial C:N ratio and $\delta^{13}C$ values in the POM, and the strong correlations between high turbidity and increased concentrations of DTotHg (Spearman's rank correlation coefficient 0.5; *p*-value <0.01) and PartTotHg (Spearman's rank correlation coefficient 0.7; p-value <0.01) in surface water during the run-off period, in addition to very low salinity (ranging from 0.18 to 15.7 PSU, Fig. S1 in the Supplementary material), demonstrates that inputs from the Adventelva River are a source of Hg to the fjord, and have the potential to affect zooplankton food-sources and contaminant exposure.

4.1.1. Effects of river inputs on POM composition in Adventfjorden

POM composition in Adventfjorden varied through the summer melt season. Changes in C:N ratios and stable $\delta^{13}C$ and $\delta^{15}N$ values of the POM suggest a transition from detritus and heterotrophs in the pre-bloom phase to phytoplankton during the spring bloom in May, followed by a strong contribution of terrestrial particles when river discharge increased during the late summer period.

Since Adventfjorden is a relatively small fjord (~7 km from the river outlet to the fjord mouth), the river plume impacts the entire fjord at certain times of the year such as during peak runoff, (after rainstorms and/or melting events) leading to the dispersal of terrestrial matter throughout the entire fjord (Walch et al., 2022). This is consistent with our finding that seasonal changes in POM overwhelmed spatial differences within the fjord, which highlights the dynamic nature of this estuarine system.

In this study, April represents pre-bloom conditions in Adventfjorden, when the coast was icy but the fjord (including the inner fjord) was ice free. Degradation of organic material by bacteria can lead to increased $\delta^{15}N$ of POM, since consumers are enriched in $\delta^{15}N$ relative to their diet (Hoch et al., 1996; Søreide et al., 2006) and pelagic POM from detritus-rich waters also tends to be enriched in $\delta^{15}N$ (Søreide et al., 2006). Thus, the high $\delta^{15}N$ values in the water column in April (ranging from 4.4 to 6.8 ‰) indicate that POM was mainly composed of heterotrophic organisms and detritus at this time.

In May, stable isotope composition of POM reflected the presence of phytoplankton in the water column from the diatom dominating spring bloom, which peaked 10 days before the sampling in May. The Adventelva River was open and running in May, but water levels were low and the water was clear (N. Carrasco, pers. obs.). Thus, these inputs were not observed in the carbon signatures in Adventfjorden, where surface water DOM (McGovern et al., 2020a) and POM (this study) characteristics were dominated by marine phytoplankton with $\delta^{13}C$ ranging from −25.6 to −22.8 ‰ (bloom timing date based on Nyeggen (2019)), which typically are more enriched compared to terrestrial carbon sources (De La Vega et al., 2019). These high $\delta^{13}C$ values, together with increases in Chl-*a* concentrations from April to May (from 0.1 ± 0.06 μg/L in April to 0.6 ± 0.2 μg/L in May) and relatively low molar C:N ratios (ranging from 4.5 to 13 in May) confirm that phytoplankton dominated the POM at this time. Low C:N ratios are typically observed where phytoplankton contribution to the POM is high, and where N is not limiting (Bates et al., 2005; Søreide et al., 2006). In contrast, high C:N ratios are typical of systems strongly influenced by terrestrial organic matter inputs (Koziorowska et al., 2016). Thus, the increase in C:N ratio from May to June, that we observed in Adventfjorden POM can be attributed to increases in turbid freshwater inputs. POC:Chl-*a* ratio which is also used to identify POM samples dominated by marine phytoplankton (Liénart et al., 2017), followed the same trend as C:N ratio, with the highest values in June and July inner fjord (3400 and 8300 respectively) and lowest values in April and May (ranging from 231 to 1600).

Freshwater inputs from the Adventelva River in June, July and August were rich in terrestrial sediments and organic matter. The high POM C:N ratios observed in surface waters from the inner fjord in June and July in addition to the lower $\delta^{15}N$ and $\delta^{13}C$ values in POM in June, July and August (similar to riverine values), suggest a much greater contribution of terrestrial particles to the POM during peak river discharge. The relatively consistent Chl-*a* concentrations across stations and dates, despite very low light availability in the inner fjord during the summer months, likely reflects the delivery of marine-advected phytoplankton to Adventfjorden throughout the summer (as also observed by Kubiszyn et al., 2017).

4.1.2. Effects of river inputs on Hg concentration in Adventfjorden

The Adventelva River was an important source of Hg to Adventfjorden during the summer period. DTotHg concentrations in river water were lower than concentrations found in several major Arctic rivers, including the Yenisei, Ob, Lena and Mackenzie rivers (Adventelva River: 0.3 ± 0.3 ng/L; Yenisei: 0.65 ng/L; Ob: 1.31 ng/L; Lena: 2.19 ng/L and Mackenzie: 1.61 ng/L; Coquery et al., 1995; Leitch et al., 2007; Outridge et al., 2008; Søndergaard et al., 2012). PartTotHg concentrations in the Adventelva River (ranging from 7 to 13 ng/L) increased over the summer season from May to August, and were overall higher than concentrations found in other Arctic rivers (Mackenzie: 3.68 ng/L, Nelson: 0.33 ng/L, Hayes 1.07 ng/L; Hare et al., 2008; Leitch et al., 2007; Søndergaard et al., 2012). However, when normalized by SPM, TotHg concentrations fall within the range observed in these rivers (Adventelva River: 58 ± 7 ng/g; Yenisei: 66 ng/g; Ob: 53 ng/g; Lena: 140 ng/g and Mackenzie: 13 ng/g; Outridge et al., 2008; Coquery et al., 1995; Leitch et al., 2007).

The main source of Hg to the Adventelva River is atmospheric deposition in the catchment following long-range transport (Halbach et al., 2017; Aslam et al., 2019). However, local Hg deposits may have been created in the beginning of the 20th century when Longyearbyen was one of several coal mining camps in Svalbard (Hoel, 1938). Higher concentrations have been reported in the vegetated layer compared to the deeper soil horizons (Aslam et al., 2019), strongly related to organic matter concentrations (Halbach et al., 2017; Kim et al., 2020). The observed seasonality in Hg concentrations in river water samples reflects these seasonal changes in organic carbon concentrations. DTotHg concentrations in the Adventelva River were highest during the snowmelt period in May, when DOC concentrations were 10-fold higher than in June and August (McGovern et al., 2020a). Previous studies from Arctic rivers have highlighted the importance of spring freshet in delivering DOM (Amon et al., 2012; Kaiser et al., 2017) as well as DOM-associated Hg as meltwater follows shallow flow paths through the catchment to the river (Zhang et al., 2015). In addition, snowmelt may be a source of atmospheric Hg. Studies from Ny-Ålesund have demonstrated that snowfall is an important vector of Hg deposition on Svalbard, and that during snow-melt in springtime, reactive Hg takes a more stable form as it interacts with organic matter, and that the melting process may be an important avenue for atmospheric Hg to enter aquatic systems (Ferrari et al., 2008). In contrast to Hg in the dissolved phase, PartTotHg concentrations were higher later in the summer, with a peak in July, likely increasing with POC concentrations as the active layer deepens and erosional transport from the catchment increases.

Hg concentrations in fjord surface waters reflected the trends in

riverine inputs, suggesting that the river was a main source of Hg to the fjord, as it is the case for much of the coastal Arctic (Zolkos et al., 2020) where Hg concentrations in surface water demonstrate strong seasonality linked to seasonal ice melt and river inputs from large Arctic rivers (Dastoor et al., 2022; Emmerton et al., 2013; Leitch et al., 2007). After the pulse of snowmelt DTotHg in May, the TotHg pool was dominated by PartTotHg (0.1–8.1 ng/L) through July and August. This is likely due to the low concentrations of DOC in the Adventelva River later in the season, when the dominant form of OM is particulate. Indeed, most riverine Hg is transported to the ocean associated with particles (Liu et al., 2021; Sonke et al., 2018; Emmerton et al., 2013; Schuster et al., 2011). In Adventfjorden surface waters, %PartTotHg concentrations ranged from 41 % to 93 % over the summer, which are similar values to those reported for other river influenced coastal areas such as the Mackenzie Delta (ranging from 66 % to 74 %; Leitch et al., 2007). However, during the early part of the season, when river inputs are extremely low, Hg in seawater is much more likely to be derived from long-range atmospheric and oceanic transport of Hg. The mean Hg concentration found in the core water of the West Spitsbergen Current (0.80 ± 0.26 pM ~ 0.16 ng/L) (Petrova et al., 2020) is in the same range as aqueous Hg values found in Adventfjorden in April and the outer fjord over the summer period (0.1–0.2 ng/L).

4.2. Seasonal variability in zooplankton diet and Hg contamination

Based on FATM (Figs. 4 & 6), we observed a shift in zooplankton diet over the study period. In April, the relatively high proportion of SFA (31.9 ± 3.8 %), MUFA (36.9 ± 1.9 %) and bacteria markers (1.65 ± 0.9 %), suggest that zooplankton were mainly feeding on heterotrophs. Then in May, during the bloom, they mainly relied on diatoms (23.11 ± 5.1 %). During the summer period from June to August, zooplankton continued to mainly feed on phytoplankton, this is reflected in the relatively high proportion of dinoflagellates and PUFA markers over this period (ranging respectively from 31.8 to 38.30 %; and from 40.8 to 62.2 %). In addition, terrestrial carbon source as well as bacteria were detected in their diet during the river runoff as observed with the increase of terrestrial and bacteria markers over the summer (ranging respectively from 0.07 to 0.6 %; and from 0.6 to 2.4 %).

Our observations of utilization of terrestrial energy sources by fjord zooplankton during the main river discharge period are consistent with other studies that have shown the use of terrestrial carbon by coastal biota (Bell et al., 2016; Harris et al., 2018; McGovern et al., 2020b). Zooplankton can take up terrestrial OM either directly or indirectly through the microbial loop, whereby organic matter from river inputs is utilized by bacteria, which are grazed on by ciliates, heterotrophic nanoflagellates and rotifers, and then transferred to larger zooplankton (Rysgaard and Nielsen, 2006; McMeans et al., 2015).

When studying an ecosystem with several carbon sources (e.g. marine vs. terrestrial), it is important to consider the strong variability in $\delta^{13}C$ and $\delta^{15}N$ at the base of the food web (Post, 2002). In this study, the similar seasonality in $\delta^{13}C$ and $\delta^{15}N$ for zooplankton and POM suggests that the bulk POM changes from a strong contribution of heterotrophs (April) to phytoplankton (May–June) to terrestrial particles (July–August) are mirrored in the zooplankton. Indeed, $\delta^{13}C$ values in zooplankton found in May–June correspond to previously reported values of zooplankton feeding on phytoplankton (i.e. diatoms with $\delta^{13}C$ values ranging from −19 ‰ to −15 ‰) (Post, 2002; Fry and Wainwright, 1991) (which is also consistent with FA markers), whereas $\delta^{13}C$ values in zooplankton found in July–August suggest a diet mixing dinoflagellates with a lower $\delta^{13}C$ value (ranging from −22 ‰ to −20 ‰) (Fry and Wainwright, 1991) than diatoms (Brandenburg et al., 2022), and terrestrial material with $\delta^{13}C$ values typically around −28 ‰ (Kuzyk et al., 2010). The larger magnitude of the change in stable isotope values for POM than in zooplankton samples can partly be explained by the longer tissue turnover time for marine invertebrates than, for example, phytoplankton or bacteria, leading to a delayed response to changes in the $\delta^{13}C$ and $\delta^{15}N$ relative to their prey. But it also can be explained by the fact that zooplankton can buffer against a shift from phytoplankton dominating the POM to terrestrial particles dominating the POM through selective feeding. The enrichment in $\delta^{13}C$ of zooplankton relative to POM over the study can be explained by the fact that POM is a mix of detritus, phytoplankton, heterotrophs, and bacteria (Rau et al., 1990), while many zooplankton taxa are selective feeders (DeMott, 1988; Paffenhöfer, 1988) and preferably feed on higher $\delta^{13}C$ sources such as phytoplankton (Søreide et al., 2006). Although lipid correction of $\delta^{13}C$ values in zooplankton was applied in order to limit the effect of seasonal and interspecific differences in lipid concentration, this method may have led to over-enrichment in May samples when meroplankton (with lower lipid content) were dominant, compared to July and August when *Calanus* sp. dominated the zooplankton samples.

The seasonal variation in zooplankton community structure described in this study, is a typical pattern also observed in other coastal areas in Svalbard (Walkusz et al., 2009; Lischka and Hagen, 2016), with some species being present throughout the sampling period (e.g. *Calanus* spp.). All zooplankton samples were largely dominated by species known to be mainly herbivorous and omnivorous. The largest size fraction (> 500 μm) was dominated by *Calanus* spp. during the entire study period (except in May, when it was dominated by decapod zoea). Calanoid copepods, which are known to be selective suspension feeders, have been found to include terrestrial energy sources in their diet in freshwater systems when phytoplankton availability is low relative to allochthonous particles (Berggren et al., 2014; Poste et al., 2019) and this may also occur in the marine environment. The use of allochthonous energy sources rather than phytoplankton during the summer months may have implications for Hg bioaccumulation and biomagnification in zooplankton because it is a lower quality food source and is associated with higher Hg contamination (Hiltunen et al., 2019; Jonsson et al., 2017). Further, the microbial food web has more trophic levels, and therefore allows for increased biomagnification (Jonsson et al., 2017).

Zooplankton samples dominated by *Calanus* spp. (> 500 μm) collected in June, July and August displayed lower mean TotHg and MeHg concentrations (9.1 ± 1.1 ng/g and 1.5 ± 1.0 ng/g respectively) compared to *Calanus* spp. samples collected in pan-arctic coastal and open marine systems, such as the Laptev Sea, the Hudson Bay, the Canadian Arctic Archipelago, the southern Beaufort Sea, the Chukchi Sea, or the Northern Baffin Bay with mean TotHg and MeHg concentrations ranging from 7 to 32 ng/g and from 3 to 11 ng/g respectively (Loseto et al., 2008; Foster et al., 2012; Pomerleau et al., 2016). They also displayed much lower mean TotHg and MeHg concentrations compared to *Gammarus setosus* sampled in the inner area of Adventfjord influenced by Adventelva River discharge in the same period (Hg: 20.2 ± 2.9 ng/g dw; MeHg: 5.8 ± 4.6 ng/g dw) (Skogsberg et al., 2022). The proportion of Hg present as MeHg (%MeHg) in zooplankton from Adventfjorden (10 ± 7 %) was much lower than values reported from Hudson Bay for *Calanus* spp. (24 ± 16 %) and the Southern Beaufort Sea (42 ± 16 %) (Pomerleau et al., 2016), but in the same range as the Baffin Bay (7.5 %; Campbell et al., 2005) and the Barents Sea (6–9 %; Joiris et al., 1995). The relatively low %MeHg values may reflect mainly exposure to inorganic mercury delivered from land.

The lack of a spatial gradient in zooplankton TotHg and MeHg concentrations across the fjord can be explained by fjord dynamics, with water currents, tides and advection processes moving zooplankton around the fjord.

Seasonal changes in Hg in zooplankton could be attributed to several potential main drivers: 1) changes in zooplankton community composition (including changes in developmental stages), 2) changes in zooplankton diet, and 3) changes in abiotic Hg concentrations. The increase of Hg in zooplankton over the study period could be explained by a shift in developmental stages within zooplankton communities, with older stages displaying higher concentration in TotHg than younger stages. Among *Calanus* spp. individuals, seasonal variability was observed in the proportion of developmental stages, with a higher mean

proportion of CV stages in July and August (70 ± 26 % and 79 ± 12 % respectively) than during the previous months (43 ± 32 % in June and 50 ± 20 % in April) and a decrease in the mean proportion in CIV stages present from June to August (45 ± 26 %, 24 ± 19 % and 13 ± 8 % respectively). However, published data on Hg accumulation dynamics by developmental stage for zooplankton are rare, likely in part due to concurrent changes in diet and/or growth dynamics that are also likely to impact Hg concentrations.

Diet is the most important pathway for TotHg uptake by zooplankton (Lawson and Mason, 1998; Lee and Fisher, 2017; Schartup et al., 2018). Although in this study phytoplankton (diatoms in May and dinoflagellates during the summer) was the main food source for zooplankton, even during the main river discharge period, several studies have observed that in estuarine locations influenced by terrestrial organic matter inputs, MeHg uptake by phytoplankton may be reduced due to strong sorption of MeHg to terrestrial organic matter with low bioavailability (Schartup et al., 2015a, 2018). Thus, zooplankton may have taken up MeHg from another diet source. The ingestion of heterotrophic organisms can increase MeHg bioaccumulation in microzooplankton, mesozooplankton and macrozooplankton (Kainz et al., 2006; Pomerleau et al., 2016). In addition, several studies in boreal lakes (Poste et al., 2019; Wu et al., 2019) and estuaries (Jonsson et al., 2017) have described how terrestrial inputs can enhance MeHg concentration in water and in zooplankton that include terrestrial energy sources in their diet. In this study, the relatively high proportion of heterotrophic dietary markers in zooplankton with higher terrestrial and bacterial dietary markers during the summer period, in addition to the low $\delta^{13}C$ values observed in July and August and the positive correlation with the dinoflagellate and bacteria FATM suggest that direct and indirect terrestrial carbon source (uptake of terrestrial POC and uptake of bacteria relying on terrestrial DOC respectively) included in zooplankton diet may explain the increase in Hg concentration over the summer (Fig. 7).

The earlier increase in TotHg concentration in zooplankton compared to MeHg, in addition to the relatively low %MeHg ratio in May and June compared to the summer, could be explained by rivers bringing large amounts of inorganic Hg in melt water and thus increasing zooplankton exposure to inorganic Hg. This is consistent with the positive correlation between the TotHg concentration in zooplankton with surface water turbidity, PartTotHg and DTotHg concentrations. The delayed increase of MeHg concentrations and the highest %MeHg in July and August, could be explained by an increased exposure to MeHg due to higher methylation during summer, where fresh organic matter (including from marine phytoplankton), river inputs of inorganic Hg, and higher temperature can promote methylation in the water column (Schuster et al., 2011; Schartup et al., 2015b). In addition to dietary uptake of MeHg, zooplankton are also known to accumulate MeHg via diffusion from the surrounding water, with some studies indicating that diffusion can account for 10–20 % of total uptake (Kim and Burggraaf, 1999; Lee and Fisher, 2017). Therefore, while TotHg concentrations in zooplankton in our study seemed to be more strongly linked to river inputs, our results suggest that MeHg concentrations may be more strongly driven by zooplankton developmental stage- and diet. This is also supported by the negative correlation between MeHg concentration and $\delta^{13}C$ in zooplankton samples and the positive correlation between DTotHg in water samples and TotHg concentration in zooplankton samples.

In the context of climate change, warmer air temperatures will lead to accelerated permafrost thaw and increased frequency of high river flow events, with more Hg and carbon mobilized and released into Arctic rivers and estuaries, as well as water temperature increase leading to faster methylation rates (Yang et al., 2016). This will increase Hg and MeHg exposure to zooplankton in coastal waters. Increased river discharge may also increase turbidity in estuaries, promoting microbial

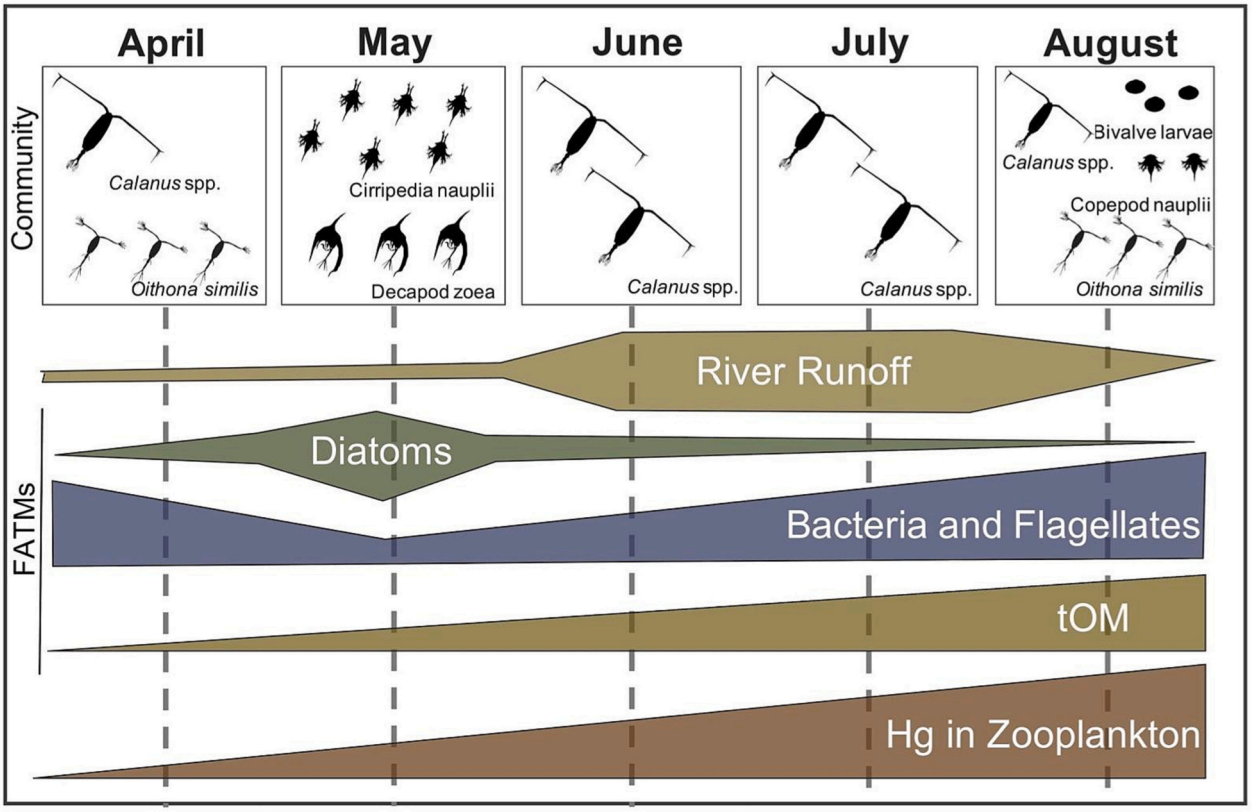

Fig. 7. Conceptual figure summarizing shifts in zooplankton community structure from April to August 2018 alongside changes in zooplankton fatty acid trophic markers (FATM) and concentrations of Hg.

activity, rather than phytoplankton production, thus increasing food chain length, altering food quality at the food web base and potentially enhancing Hg bioaccumulation and biomagnification. However, it remains challenging to assess the potential net impacts of co-occurring changes in Hg exposure, productivity, plankton community structure, and food web interactions on Hg concentrations in Arctic coastal zooplankton, in particular given the additional complexity associated with the strong seasonality characteristic of Arctic terrestrial and marine ecosystems.

5. Conclusion

Given the expected increases in river discharge, including the transport of Hg from permafrost catchments to coastal areas, there is a need for understanding how terrestrial inputs are likely to affect uptake and trophic transfer of Hg in marine food webs. Our results indicate that river inputs can lead to increased Hg exposure for coastal food webs, while utilization of terrestrial and heterotrophic carbon sources by zooplankton during the main discharge period may be linked to increased bioaccumulation of Hg. This study, by following zooplankton through the summer melt season, highlights the effects of river runoff on surface water physicochemistry, zooplankton diet, and the bioaccumulation of TotHg and MeHg in Arctic coastal waters, while also demonstrating the importance of high resolution temporal studies for understanding Hg dynamics in highly seasonal Arctic coastal food webs.

CRediT authorship contribution statement

Nathalie Carrasco: Conceptualization, Methodology, Formal analysis, Investigation, Visualization, Writing – original draft. **Maeve McGovern**: Conceptualization, Methodology, Formal analysis, Investigation, Graphical abstract, Visualization, Writing - review & editing, Funding acquisition. **Anita Evenset**: Conceptualization, Methodology, Writing – review & editing, Supervision. **Janne E. Søreide**: Conceptualization, Methodology, Resources, Writing – review & editing, Supervision. **Sofi Jonsson**: Investigation, Writing – review & editing. **Michael Arts**: Investigation, Writing – review & editing. **Amanda Poste**: Initial conceptualization, Methodology, Resources, Supervision, Investigation, Writing – Review & editing, Project administration, Funding acquisition.

Declaration of competing interest

The authors declare that they have no known competing financial interests or personal relationships that could have appeared to influence the work reported in this paper.

Data availability

Data will be made available on request.

Acknowledgements

We thank T. Brytensen, HF. Braaten and E. Skogsberg for MeHg analyses, Dino Milotic and Ben Schultz (Toronto Metropolitan University) for fatty acid analyses, and M. Marquardt for Chlorophyll-*a* analysis, A. L. Ribeiro, T. Brytensen, H. F. Veiteberg Braaten for TotHg analysis (NIVA lab), the UC Davis Stable Isotope Facility, in California (USA) for running the stable isotope analysis, and E. Skogsberg, E. Vereide and C. Ugelstad for help in the field. This project was funded by the Norwegian Research Council (TerrACE; project number: 268458) and the Svalbard Science Forum (Arctic Field Grant; RIS number: 10914).

Appendix A. Supplementary data

Supplementary data to this article can be found online at https://doi.org/10.1016/j.scitotenv.2023.167643.

References

AMAP, 2021. AMAP Assessment 2021: Mercury in the Arctic. Arctic Monitoring and Assessment Programme (AMAP), Tromsø, Norway, p. 324.
Amon, R., Rinehart, A., Duan, S., et al., 2012. Dissolved organic matter sources in large arctic rivers. Geochim. Cosmochim. Acta 94, 217–237.
Andersson, A., Brugel, S., Paczkowska, J., Rowe, O.F., Figueroa, D., Kratzer, S., Legrand, C., 2018. Influence of allochthonous dissolved organic matter on pelagic basal production in a northerly estuary. Estuar. Coast. Shelf Sci. 204, 225–235.
Ariya, P.A., Dastroor, A.P., Amyot, M., et al., 2004. The arctic: a sink for mercury. Tellus Ser. B Chem. Phys. Meteorol. 56, 397–403.
Arts, M.T., Brett, M.T., Kainz, M.J., 2009. Lipids in Aquatic Ecosystems. https://doi.org/10.1007/978-0-387-89366-2.
Aslam, S.N., Huber, C., Asimakopoulos, A.G., Steinnes, E., Mikkelsen, Ø., 2019. Trace elements and polychlorinated biphenyls (PCBs) in terrestrial compartments of svalbard, norwegian arctic. Sci. Total Environ. 685, 1127–1138.
Bates, N.R., Best, M.H., Hansell, D.A., 2005. Spatio-temporal distribution of dissolved inorganic carbon and net community production in the chukchi and Beaufort seas. Deep-Sea Res. II Top. Stud. Oceanogr. 52, 3303–3323.
Bell, L.E., Bluhm, B.A., Iken, K., 2016. Influence of terrestrial organic matter in marine food webs of the Beaufort Sea shelf and slope. Mar. Ecol. Prog. Ser. 550, 1–24.
Berggren, M., Ziegler, S.E., St-Gelais, N.F., Beisner, B.E., Del Giorgio, P.A., 2014. Contrasting patterns of allochthony among three major groups of crustacean zooplankton in boreal and temperate lakes. Ecology 95, 1947–1959.
Blachowiak-Samolyk, K., Søreide, J.E., Kwasniewski, S., Sundfjord, A., Hop, H., Falk-Petersen, S., Hegseth, E.N., 2008. Hydrodynamic control of mesozooplankton abundance and biomass in northern svalbard waters (79–81 n). Deep-Sea Res. II Top. Stud. Oceanogr. 55, 2210–2224.
Bodin, N., Le Loc'h, F., Hily, C., 2007. Effect of lipid removal on carbon and nitrogen stable isotope ratios in crustacean tissues. J. Exp. Mar. Biol. Ecol. 341, 168–175.
Braaten, H.F.V., de Wit, H.A., Fjeld, E., Rognerud, S., Lydersen, E., Larssen, T., 2014. Environmental factors influencing mercury speciation in subarctic and boreal lakes. Sci. Total Environ. 476, 336–345.
Brandenburg, K.M., Rost, B., Van de Waal, D.B., Hoins, M., Sluijs, A., 2022. Physiological control on carbon isotope fractionation in marine phytoplankton. Biogeosciences 19, 3305–3315.
Campbell, L.M., Norstrom, R.J., Hobson, K.A., Muir, D.C., Backus, S., Fisk, A.T., 2005. Mercury and other trace elements in a pelagic arctic marine food web (northwater polynya, baffin bay). Sci. Total Environ. 351, 247–263.
Clarkson, T.W., Magos, L., Myers, G.J., 2003. The toxicology of mercury—current exposures and clinical manifestations. N. Engl. J. Med. 349, 1731–1737.
Coquery, M., Cossa, D., Martin, J., 1995. The distribution of dissolved and particulate mercury in three siberian estuaries and adjacent arctic coastal waters. Water Air Soil Pollut. 80, 653–664.
Dastoor, A., Angot, H., Bieser, J., Christensen, H.H., Dougles, T.A., Heimbürger-Boavida, L.-E., Jiskra, M., Mason, R.P., McLagan, D.S., Obrist, D., Outridge, P.M., Petrova, M.V., Ryjkov, A., St, K.A., Pierre, A.T., Schartup, A.L., Soerensen, K., Toyota, O., Travnikov, S.J., Wilson, C. Zdanowicz, 2022. Arctic mercury cycling. Nature Reviews Earth & Environment 3, 270–286.
De La Vega, C., Jeffreys, R.M., Tuerena, R., Ganeshram, R., Mahaffey, C., 2019. Temporal and spatial trends in marine carbon isotopes in the arctic ocean and implications for food web studies. Glob. Chang. Biol. 25, 4116–4130.
DeMott, W.R., 1988. Discrimination between algae and detritus by freshwater and marine zooplankton. Bull. Mar. Sci. 43, 486–499.
Dommergue, A., Ferrari, C.P., Gauchard, P.-A., Boutron, C.F., Poissant, L., Pilote, M., Jitaru, P., Adams, F.C., 2003. The fate of mercury species in a sub-arctic snowpack during snowmelt. Geophys. Res. Lett. 30.
Emmerton, C.A., Graydon, J.A., Gareis, J.A., St, V.L., Louis, L.F., Lesack, J.K., Banack, F. Hicks, Nafziger, J., 2013. Mercury export to the arctic ocean from the mackenzie river, Canada. Environ. Sci. Technol. 47, 7644–7654.
Ferrari, C.P., Padova, C., Faïn, X., et al., 2008. Atmospheric mercury depletion event study in ny-alesund (svalbard) in spring 2005. Deposition and transformation of hg in surface snow during springtime. Sci. Total Environ. 397, 167–177.
Folch, J., Lees, M., Sloane Stanley, G.H., et al., 1957. A simple method for the isolation and purification of total lipids from animal tissues. J. Biol. Chem. 226, 497–509.
Foster, K.L., Stern, G.A., Pazerniuk, M.A., Hickie, B., Walkusz, W., Wang, F., Macdonald, R.W., 2012. Mercury biomagnification in marine zooplankton food webs in Hudson bay. Environ. Sci. Technol. 46, 12952–12959.
Fry, B., Wainwright, S.C., 1991. Diatom sources of 13C-rich carbon in marine food webs. Mar. Ecol. Prog. Ser. 76, 149–157.
Gagnon, C., Pelletier, E., Mucci, A., Fitzgerald, W.F., 1996. Diagenetic behavior of methylmercury in organic-rich coastal sediments. Limnol. Oceanogr. 41, 428–434.
Gilmour, C.C., Podar, M., Bullock, A.L., Graham, A.M., Brown, S.D., Somenahally, A.C., Johs, A., Hurt Jr., R.A., Bailey, K.L., Elias, D.A., 2013. Mercury methylation by novel microorganisms from new environments. Environ. Sci. Technol. 47 (20), 11810–11820. https://doi.org/10.1021/es403075t.
Halbach, K., Mikkelsen, Ø., Berg, T., Steinnes, E., 2017. The presence of mercury and other trace metals in surface soils in the norwegian arctic. Chemosphere 188, 567–574.
Hall, B., Bodaly, R., Fudge, R., Rudd, J., Rosenberg, D., 1997. Food as the dominant pathway of methylmercury uptake by fish. Water Air Soil Pollut. 100, 13–24.

Hare, A., Stern, G.A., Macdonald, R.W., Kuzyk, Z.Z., Wang, F., 2008. Contemporary and preindustrial mass budgets of mercury in the Hudson Bay marine system: the role of sediment recycling. Sci. Total Environ. 406, 190–204.
Harris, C.M., McTigue, N.D., McClelland, J.W., Dunton, K.H., 2018. Do high arctic coastal food webs rely on a terrestrial carbon subsidy? Food Webs 15, e00081.
Hessen, D.O., Carroll, J., Kjeldstad, B., Korosov, A.A., Pettersson, L.H., Pozdnyakov, D., Sørensen, K., 2010. Input of organic carbon as determinant of nutrient fluxes, light climate and productivity in the Ob and yenisey estuaries. Estuar. Coast. Shelf Sci. 88, 53–62.
Hiltunen, M., Peltomaa, E., Brett, M.T., Aalto, S.L., Strandberg, U., Oudenampsen, J., Burgwal, L.M., Taipale, S.J., 2019. Terrestrial organic matter quantity or decomposition state does not compensate for its poor nutritional quality for daphnia. Freshw. Biol. 64, 1769–1786. https://doi.org/10.1111/fwb.13368.
Hintelmann, H., Nguyen, H.T., 2005. Extraction of methylmercury from tissue and plant samples by acid leaching. Anal. Bioanal. Chem. 381, 360–365.
Hobson, K.A., Clark, R.G., 1992. Assessing avian diets using stable isotopes I: turnover of 13C in tissues. Condor 94, 181–188.
Hoch, M.P., Snyder, R.A., Cifuentes, L.A., Coffin, R.B., 1996. Stable isotope dynamics of nitrogen recycled during interactions among marine bacteria and protists. Mar. Ecol. Prog. Ser. 132, 229–239.
Hoel, A., 1938. Coal-mining in Svalbard. Polar Record 2 (16), 74–85.
Holm-Hansen, O., Riemann, B., 1978. Chlorophyll a determination: improvements in methodology. Oikos 438–447.
Joiris, C., Ali, I., Holsbeek, L., Bossicart, M., Tapia, G., 1995. Total and organic mercury in barents sea pelagic fish. Bull. Environ. Contam. Toxicol. 55, 674–681.
Jonsson, S., Andersson, A., Nilsson, M.B., Skyllberg, U., Lundberg, E., Schaefer, J.K., Åkerblom, S., Björn, E., 2017. Terrestrial discharges mediate trophic shifts and enhance methylmercury accumulation in estuarine biota. Sci. Adv. 3, e1601239.
Kainz, M., Telmer, K., Mazumder, A., 2006. Bioaccumulation patterns of methyl mercury and essential fatty acids in lacustrine planktonic food webs and fish. Sci. Total Environ. 368, 271–282.
Kaiser, K., Canedo-Oropeza, M., McMahon, R., Amon, R.M., 2017. Origins and transformations of dissolved organic matter in large arctic rivers. Sci. Rep. 7, 1–11.
Kim, H., Kwon, S.Y., Lee, K., et al., 2020. Input of terrestrial organic matter linked to deglaciation increased mercury transport to the svalbard fjords. Sci. Rep. 10, 1–11.
Kim, J.P., Burggraaf, S., 1999. Mercury bioaccumulation in rainbow trout (oncorhynchus mykiss) and the trout food web in lakes okareka, okaro, tarawera, rotomahana and rotorua, New Zealand. Water Air Soil Pollut. 115, 535–546.
Koziorowska, K., Kuliński, K., Pempkowiak, J., 2016. Sedimentary organic matter in two spitsbergen fjords: terrestrial and marine contributions based on carbon and nitrogen contents and stable isotopes composition. Cont. Shelf Res. 113, 38–46.
Kubiszyn, A., Wiktor, J., Wiktor Jr., J., Griffiths, C., Kristiansen, S., Gabrielsen, T., 2017. The annual planktonic protist community structure in an ice-free high arctic fjord (adventfjorden, west spitsbergen). J. Mar. Syst. 169, 61–72.
Kuhnlein, H.V., Chan, H.M., 2000. Environment and contaminants in traditional food systems of northern indigenous peoples. Annu. Rev. Nutr. 20, 595–626.
Kuzyk, Z.Z.A., Macdonald, R.W., Tremblay, J.-E., Stern, G.A., 2010. Elemental and stable isotopic constraints on river influence and patterns of nitrogen cycling and biological productivity in Hudson Bay. Cont. Shelf Res. 30 (2), 163–176.
Lawson, N.M., Mason, R.P., 1998. Accumulation of mercury in estuarine food chains. Biogeochemistry 40, 235–247.
Lee, C.-S., Fisher, N.S., 2017. Bioaccumulation of methylmercury in a marine copepod. Environ. Toxicol. Chem. 36, 1287–1293.
Lehnherr, I., 2014. Methylmercury biogeochemistry: a review with special reference to arctic aquatic ecosystems. Environ. Rev. 22, 229–243.
Leitch, D.R., Carrie, J., Lean, D., Macdonald, R.W., Stern, G.A., Wang, F., 2007. The delivery of mercury to the Beaufort Sea of the arctic ocean by the mackenzie river. Sci. Total Environ. 373, 178–195.
Liénart, C., Savoye, N., Bozec, Y., Breton, E., Conan, P., David, V., Lebreton, B., 2017. Dynamics of particulate organic matter composition in coastal systems: a spatio-temporal study at multi-systems scale. Prog. Oceanogr. 156, 221–239. https://doi.org/10.1016/j.pocean.2017.03.001.
Lim, A.G., Jiskra, M., Sonke, J.E., Loiko, S.V., Kosykh, N., Pokrovsky, O.S., 2020. A revised northern soil hg pool, based on western Siberia permafrost peat hg and carbon observations. Biogeosciences 17, 3083–3097.
Lischka, S., Hagen, W., 2016. Seasonal dynamics of mesozooplankton in the Arctic Kongsfjord (Svalbard) during year-round observations from august 1998 to July 1999. Polar Biol. 39, 1859–1878. https://doi.org/10.1007/s00300-016-2005-z.
Liu, M., Zhang, Q., Maavara, T., Liu, S., Wang, X., Raymond, P.A., 2021. Rivers as the largest source of mercury to coastal oceans worldwide. Nat. Geosci. 14 (9), 672–677.
Loseto, L., Stern, G., Deibel, D., Connelly, T., Prokopowicz, A., Lean, D., Fortier, L., Ferguson, S., 2008. Linking mercury exposure to habitat and feeding behaviour in Beaufort Sea beluga whales. J. Mar. Syst. 74, 1012–1024.
Macdonald, R., Loseto, L., 2010. Are arctic ocean ecosystems exceptionally vulnerable to global emissions of mercury? A call for emphasised research on methylation and the consequences of climate change. Environ. Chem. 7, 133–138.
McGovern, M., Evenset, A., Borgå, K., et al., 2019. Implications of coastal darkening for contaminant transport, bioavailability, and trophic transfer in northern coastal waters.Environmental science &. Technology. 53 (13), 7180–7182.
McGovern, M., Pavlov, A.K., Deininger, A., Granskog, M.A., Leu, E., Søreide, J.E., Poste, A.E., 2020a. Terrestrial inputs drive seasonality in organic matter and nutrient biogeochemistry in a high arctic fjord system (isfjorden, svalbard). Front. Mar. Sci. 7, 747.
McGovern, M., Poste, A.E., Oug, E., Renaud, P.E., Trannum, H.C., 2020b. Riverine impacts on benthic biodiversity and functional traits: a comparison of two sub-arctic fjords. Estuar. Coast. Shelf Sci. 240, 106774.
McGovern, M., Arts, M., Borgå, K., Dąbrowska, A.M., Leu, E., Primicerio, R., Renaud, P. E., Søreide, J.E., Vereide, E.H., Poste, A.E., 2023. Turbid meltwater plumes are associated with reduced food quality for Arctic zooplankton. Manuscript in preparation for L&O. in prep.
McMeans, B.C., Koussoroplis, A.-M., Arts, M.T., Kainz, M.J., 2015. Terrestrial dissolved organic matter support growth and reproduction of Daphnia magna when algae are limiting. J. Plankton Res. 37 (6), 1201–1209. https://doi.org/10.1093/plankt/fbv083.
Morel, F.M., Kraepiel, A.M., Amyot, M., 1998. The chemical cycle and bioaccumulation of mercury. Annu. Rev. Ecol. Syst. 29, 543–566.
Nilsen, F., Cottier, F., Skogseth, R., Mattsson, S., 2008. Fjord–shelf exchanges controlled by ice and brine production: the interannual variation of Atlantic water in isfjorden, svalbard. Cont. Shelf Res. 28, 1838–1853.
Nyeggen, M.U., 2019. Seasonal Zooplankton Dynamics in Svalbard Coastal Waters: The Shifting Dominance of Mero-and Holoplankton and Timing of Reproduction in Three Species of copepoda. Master's thesis.. The University of Bergen.
Olson, C., Jiskra, M., Biester, H., Chow, J., Obrist, D., 2018. Mercury in active-layer tundra soils of Alaska: concentrations, pools, origins, and spatial distribution. Glob. Biogeochem. Cycles 32, 1058–1073.
Outridge, P., Macdonald, R., Wang, F., Stern, G., Dastoor, A., 2008. A mass balance inventory of mercury in the arctic ocean. Environ. Chem. 5, 89–111.
Paffenhöfer, G.-A., 1988. Feeding rates and behavior of zooplankton. Bull. Mar. Sci. 43, 430–445.
Parsons, T., 2013. A Manual of Chemical & Biological Methods for Seawater Analysis. Elsevier.
Petrova, M.V., Krisch, S., Lodeiro, P., Valk, O., Dufour, A., Rijkenberg, M.J.A., Achterberg, E.P., Rabe, B., van der Loeff, M.R., Hamelin, B., Sonke, J.E., Garnier, C., Heimbürger-Boavida, L.E., 2020. Mercury species export from the Arctic to the Atlantic Ocean. Mar. Chem. 103855 https://doi.org/10.1016/j.marchem.2020.103855.
Pomerleau, C., Winkler, G., Sastri, A., Nelson, R.J., Williams, W.J., 2014. The effect of acidification and the combined effects of acidification/lipid extraction on carbon stable isotope ratios for sub-arctic and arctic marine zooplankton species. Polar Biol. 37, 1541–1548.
Pomerleau, C., Stern, G.A., Pućko, M., Foster, K.L., Macdonald, R.W., Fortier, L., 2016. Pan-arctic concentrations of mercury and stable isotope ratios of carbon (^{13}C) and nitrogen (15N) in marine zooplankton. Sci. Total Environ. 551, 92–100.
Post, D.M., 2002. Using stable isotopes to estimate trophic position: models, methods, and assumptions. Ecology 83, 703–718.
Poste, A.E., Hoel, C.S., Andersen, T., Arts, M.T., Færøvig, P.-J., Borgå, K., 2019. Terrestrial organic matter increases zooplankton methylmercury accumulation in a brown-water boreal lake. Sci. Total Environ. 674, 9–18.
R Core Team, 2023. R: A Language and Environment for Statistical Computing. R Foundation for Statistical Computing, Vienna, Austria. https://www.R-project.org.
Rau, G., Teyssie, J., Rassoulzadegan, F., Fowler, S., 1990. C-13/c-12 and n-15/n-14 variations among size-fractionated marine particles-implications for their origin and trophic relationships. Mar. Ecol. Prog. Ser. 59, 33–38.
Retamal, L., Bonilla, S., Vincent, W.F., 2008. Optical gradients and phytoplankton production in the mackenzie river and the coastal Beaufort Sea. Polar Biol. 31, 363–379.
Rysgaard, S., Nielsen, T.G., 2006. Carbon cycling in a high-arctic marine ecosystem–young sound, NE greenland. Prog. Oceanogr. 71, 426–445.
Schartup, A.T., Balcom, P.H., Soerensen, A.L., Gosnell, K.J., Calder, R.S., Mason, R.P., Sunderland, E.M., 2015a. Freshwater discharges drive high levels of methylmercury in arctic marine biota. Proc. Natl. Acad. Sci. 112, 11789–11794.
Schartup, A.T., Ndu, U., Balcom, P.H., Mason, R.P., Sunderland, E.M., 2015b. Contrasting effects of marine and terrestrially derived dissolved organic matter on mercury speciation and bioavailability in seawater. Environ. Sci. Technol. 49, 5965–5972.
Schartup, A.T., Qureshi, A., Dassuncao, C., Thackray, C.P., Harding, G., Sunderland, E. M., 2018. A model for methylmercury uptake and trophic transfer by marine plankton. Environ. Sci. Technol. 52, 654–662.
Schuster, P.F., Striegl, R.G., Aiken, G.R., Krabbenhoft, D.P., Dewild, J.F., Butler, K., Kamark, B., Dornblaser, M., 2011. Mercury export from the Yukon river basin and potential response to a changing climate. Environ. Sci. Technol. 45, 9262–9267.
Schuster, P.F., Schaefer, K.M., Aiken, G.R., et al., 2018. Permafrost stores a globally significant amount of mercury. Geophys. Res. Lett. 45, 1463–1471.
Skogsberg, E., McGovern, M., Poste, A., Jonsson, S., Arts, M., Varpe, Ø., Borgå, K., 2022. Seasonal pollutant levels in littoral high-Arctic amphipods in relation to food sources and terrestrial run-off. Environ. Pollut. 306, 119361 https://doi.org/10.1016/j.envpol.2022.119361.
Skogseth, R., Olivier, L., Nilsen, F., Falck, E., Fraser, N., Tverberg, V., Ledang, A.B., Vader, A., Jonassen, M., Søreide, J., Cottier, F., Berge, J., Ivanov, B., Falk-Petersen, S., 2020. Variability and decadal trends in the Isfjorden (Svalbard) ocean climate and circulation – an indicator for climate change in the European Arctic. Prog. Oceanogr. 187, 102394.
Søndergaard, J., Rigét, F., Tamstorf, M.P., Larsen, M.M., 2012. Mercury transport in a low-arctic river in Kobbefjord, West Greenland (64 N). Water Air Soil Pollut. 223, 4333–4342.
Sonke, J.E., Teisserenc, R., Heimbürger-Boavida, L.E., Petrova, M.V., Marusczak, N., Le Dantec, T., Pokrovsky, O.S., 2018. Eurasian river spring flood observations support net Arctic Ocean mercury export to the atmosphere and Atlantic Ocean. Proc. Natl. Acad. Sci. 115 (50), E11586–E11594.
Søreide, J.E., Tamelander, T., Hop, H., Hobson, K.A., Johansen, I., 2006. Sample preparation effects on stable c and n isotope values: a comparison of methods in arctic marine food web studies. Mar. Ecol. Prog. Ser. 328, 17–28.

Walch, D.M.R., Singh, R.K., Søreide, J.E., Lantuit, H., Poste, A., 2022. Spatio-temporal variability of suspended particulate matter in a high-Arctic estuary (Adventfjorden, Svalbard) using Sentinel-2 time-series. Remote Sens. 14, 3123. https://doi.org/10.3390/rs14133123.

Walkusz, W., Kwasniewski, S., Falk Petersen, S., Hop, H., Tverberg, V., Wieczorek, P., Marcin Weslawski, J., 2009. Seasonal and spatial changes in the zooplankton community of Kongsfjorden. Svalbard. Polar Res. 28 (2), 254–281. https://doi.org/10.1111/j.1751-8369.2009.00107.x.

Wu, P., Kainz, M., Åkerblom, S., et al., 2019. Terrestrial diet influences mercury bioaccumulation in zooplankton and macroinvertebrates in lakes with differing dissolved organic carbon concentrations. Sci. Total Environ. 669, 821–832.

Yang, Z.W., Lu, X.F., Sheng, G.P., Graham, D.E., Liang, L., Wullschleger, S.D., Gu, B., 2016. Warming increases methylmercury production in an Arctic soil. Environ. Pollut. 214, 504–509.

Zajaczkowski, M., 2008. Sediment supply and fluxes in glacial and outwash fjords, Kongsfjorden and Adventfjorden. Svalbard. Polish Polar Res. 29 (1), 59–72.

Zajączkowski, M., Włodarska-Kowalczuk, M., 2007. Dynamic sedimentary environments of an Arctic glacier-fed river estuary (Adventfjorden, Svalbard). I. Flux, deposition, and sediment dynamics estuarine. Coast. Shelf Sci. 74 (1–2), 285–296.

Zajaczkowski, M., Nygard, H., Hegseth, E.N., Berge, J., 2010. Vertical flux of particulate matter in an Arctic fjord: the case of lack of the sea-ice cover in Adventfjorden 2006–2007. Polar Biol. 33 (2), 223–239.

Zhang, Y., Jacob, D.J., Dutkiewicz, S., Amos, H.M., Long, M.S., Sunderland, E.M., 2015. Biogeochemical drivers of the fate of riverine mercury discharged to the global and Arctic oceans. Glob. Biogeochem. Cycles 29, 854–864.

Zolkos, S., Krabbenhoft, D.P., Suslova, A., et al., 2020. Mercury export from arctic great rivers. Environ. Sci. Technol. 54, 4140–4148.